Letter

Exceptional ring of the buoyancy instability in stars

Armand Leclerc [1,*] Lucien Jezequel [2] Nicolas Perez [1] Asmita Bhandare [1] Guillaume Laibe [1,3,†] and Pierre Delplace [2]

[1] *Univ. Lyon, Univ. Lyon 1, Ens de Lyon, CNRS, Centre de Recherche Astrophysique de Lyon UMR5574, F-69230, Saint-Genis,-Laval, France*

[2] *Ens de Lyon, CNRS, Laboratoire de Physique, F-69342 Lyon, France*

[3] *Institut Universitaire de France, France*

(Received 25 April 2023; accepted 9 November 2023; published 11 March 2024)

We reveal properties of global modes of linear buoyancy instability in stars, characterized by the celebrated Schwarzschild criterion, using non-Hermitian topology. We identify a ring of exceptional points of order 4 that originates from the pseudo-Hermitian and pseudochiral symmetries of the system. The ring results from the merging of a dipole of degeneracy points in the Hermitian stably-stratified counterpart of the problem. Its existence is related to spherically symmetric unstable modes. We obtain the conditions for which convection grows over such radial modes. Those are met at early stages of low-mass stars formation. We finally show that a topological wave is robust to the presence of convective regions by reporting the presence of a mode transiting between the wavebands in the non-Hermitian problem, strengthening their relevance for asteroseismology.

DOI: 10.1103/PhysRevResearch.6.L012055

A fluid in a gravity field is stratified in density, and results in a stable or an unstable equilibrium. Gravity waves propagate when the stratification is stable, whereas convection develops when the equilibrium is unstable. To develop a convective layer, Sun-like stars must have reached an unstable state where the square of the buoyancy frequency is negative (Schwarzschild criterion $N^2 < 0$, [1]). Then, through the saturation of a linear instability, the star develops a quasiadiabatic convective region consisting of large-scale flows that excite waves and transport energy. In these regions, N^2 takes small negative values for convection to remain sustained, depending on its efficiency ($N^2 \simeq -0.25\,\mu\text{Hz}^2$ in the Sun [2,3]). Recently, Hermitian topology has shed light on waves propagating in stably stratified fluids [4–6], but the topology of the unstable case, which involves a non-Hermitian formalism, has not yet been studied. The topological study of waves consists of deducing simple conditions constraining the existence of particular linear modes of physical systems from topological arguments. These arguments can be expressed in a simple way, even for a complicated system of equations. Hermitian systems benefit from general topological index theorems from which one can predict the existence of modes transiting between different wavebands and quantized by a topological integer called the Chern number [7–11]. As such, Hermitian wave topology has become ubiquitous in physical fields as diverse as condensed matter [12], plasma physics [13–15], optics [16,17], materials science [18–20], or oceanography [6,21,22]. Recently, topological arguments have been used to reveal the existence of a Lamb-like wave that behaves as a gravity wave at large wavelengths but as a pressure wave at small wavelengths in stably stratified stars [4,5], raising further questions. Does this wave also propagate in convective regions, which are ubiquitous in stellar objects (e.g., Jupiter or high-mass stars, Fig. 1 of Ref. [5])? Moreover, seeds of convection in protostars have been observed recently in numerical simulations [23,24]. Figure C.1 of [23] suggests that the envelope becomes unstable to convection. Performing a linear stability analysis relative to the background reveals a few unstable radial modes whose origin have not been discussed thus far (see Fig. 1). Does topology allow for additional predictions on buoyancy instabilities in stars to further characterize the physics of the birth of convective layers? To address these questions, we study the non-Hermitian counterpart of the model derived for stellar pulsations. The search for topological properties in non-Hermitian systems has recently stimulated tremendous efforts in condensed matter [25–27], photonics [28–30], electric circuits [31], and geofluids [32] by investigating, for instance, the existence of topological edge states in non-Hermitian setups, or the appearance of peculiar degeneracy points where the wave operator becomes nondiagonalizable, called exceptional points (EPs). Here, we show that the linear perturbations of a stellar fluid with $N^2 < 0$ are described by a pseudo-Hermitian and pseudochiral symmetric theory. These symmetries constrain the eigenfrequencies and imply the presence of a ring of EPs of order 4, which is associated with unusual spherically symmetric unstable modes. Furthermore, we report the presence of modes transiting between the complex wavebands of the dispersion relation, one of which is the Lamb-like wave whose topological origin was revealed in Ref. [4], which we find to be robust to non-Hermitian $N^2 < 0$ regions.

*armand.leclerc@ens-lyon.fr
†guillaume.laibe@ens-lyon.fr

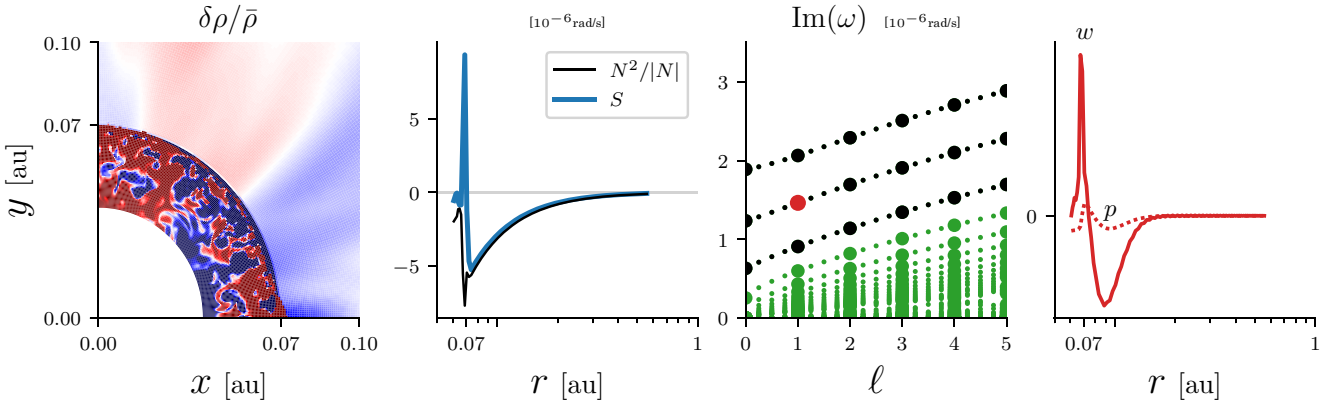

FIG. 1. First panel: Density fluctuations with respect to azimuthal average, showing convective-like motion. Data from Ref. [23] (2D simulation of an hydrodynamical stellar collapse), zoomed in near the surface of the protostar. Second panel: Average azimuthal profiles of N^2 and S, parameters involved in the linear stability analysis Eq. (2). Third and fourth panels: Growth rates of a linear stability analysis of this stratification, and profiles of pressure p and radial velocity w of one unstable mode (red), computed numerically with an eigenmodes analysis (see Ref. [33]). The instability develops both inside and outside the surface of the protostar. Three modes (black) differ from the others (green): they have nonzero growth rates on radial perturbations ($\ell = 0$).

Wave operator, wave symbol. We consider a nonmagnetic, nonrotating stellar fluid at rest in a spherically symmetric steady state. Perturbations of this equilibrium involve velocity, pressure, and density. Perturbations are adiabatic, modeling stars where the diffusion time is much longer than the dynamical time [1,34]. Perturbations of the gravitational potential are neglected (Cowling approximation [35]). The equilibrium is still static: no convection has developed yet. We discuss the superadiabatic situation at $N^2 < 0$. We define the perturbation vector $X \equiv (\tilde{v} \quad \tilde{w} \quad \tilde{\Theta} \quad \tilde{p})^\top$ based on rescaled perturbed quantities (respectively, horizontal velocity, radial velocity, entropy, and pressure), after projection onto vector spherical harmonics of angular number ℓ (see Supplemental Material (SM) [33]). The set of equations for perturbations of the form $e^{-i\omega t}X(r)$ is

$$\omega X = \mathcal{H} X, \tag{1}$$

where the *wave operator* $\mathcal{H}$ is defined as

$$\mathcal{H} \equiv \begin{pmatrix} 0 & 0 & 0 & L_\ell(r) \\ 0 & 0 & i(N^2)^{1/2} & -iS + \frac{i}{2}c_s' + ic_s\partial_r \\ 0 & -i(N^2)^{1/2} & 0 & 0 \\ L_\ell(r) & iS + \frac{i}{2}c_s' + ic_s\partial_r & 0 & 0 \end{pmatrix}. \tag{2}$$

This model involves three characteristic frequencies: the squared Brunt-Väisälä frequency

$$N^2 \equiv -g\frac{\mathrm{d}\ln\rho_0}{\mathrm{d}r} - \frac{g^2}{c_s^2}, \tag{3}$$

which characterizes buoyancy, the buoyant-acoustic frequency

$$S \equiv \frac{c_s}{2g}\left(N^2 - \frac{g^2}{c_s^2}\right) - \frac{1}{2}\frac{\mathrm{d}c_s}{\mathrm{d}r} + \frac{c_s}{r}, \tag{4}$$

which gives the rate at which buoyant and acoustic oscillations exchange momentum [5], and the squared Lamb frequency $L_\ell^2 \equiv c_s^2\,\ell(\ell+1)/r^2$, which is the momentum in the angular directions. ρ_0 is the steady background density, c_s is the speed of sound, and g is the gravity field, which are all functions of the radius r. Whenever N^2 is negative, the fluid is unstable, and the operator $\mathcal{H}$ is non-Hermitian with respect to the standard scalar product.

The spectrum of the model is obtained by solving the system of ordinary differential Eqs. (1) and (2), with appropriate boundary conditions (see SM [33]). This system implies parameters varying in space, and an analytical solution is, in general, out of reach. However, the existence of eigenmodes of $\mathcal{H}$ such as Lamb-like modes, whose frequency transits between other modes when varying a parameter (here ℓ), can be easily accessed without explicitly solving the differential system, but through topological properties of a dual *wave symbol*, a matrix H with scalar coefficients obtained by a Wigner transform of the wave operator $\mathcal{H}$ that maps the differential problem onto phase space [11], as suggested by Ref. [36]. H physically represents the local action of the medium on a plane wave, without requiring that the medium varies slowly with respect to the wavelength (see SM [33]). This symbol

matrix H reads

$$H \equiv \begin{pmatrix} 0 & 0 & 0 & L_\ell \\ 0 & 0 & iN & K_r - iS \\ 0 & -iN & 0 & 0 \\ L_\ell & K_r + iS & 0 & 0 \end{pmatrix}, \tag{5}$$

and depends on the three parameters K_r, L_ℓ, and S for fixed N^2. $K_r = c_s k_r$ with k_r the Wigner symbol of $-i\partial_r$ is the radial wave number of a wave locally plane. We denote ω and Ω the eigenvalues of $\mathcal{H}$ and H, respectively. When $N^2 > 0$, the matrix H is Hermitian and always diagonalizable with real eigenvalues. When $N^2 < 0$, N is purely imaginary and $H \neq \bar{H}^\top$.

Symmetries and exceptional points. For a subset of the parameter space (K_r, S, L_ℓ), H is nondiagonalizable. These particular points are EPs. At these points, the eigenvalues are degenerate and the eigenvectors coalesce, in the sense that the number of independent eigenvectors is less than the number of eigenvalues that merge. The occurrence of EPs is constrained by the presence of certain symmetries. In our case, one notices that H benefits from a pseudo-Hermitian symmetry

$$UHU^{-1} = \bar{H}^\top, \tag{6}$$

with the unitary transform $U = \mathrm{diag}(1, 1, -1, 1)$. Eigenvalues of pseudo-Hermitian matrices are either real or complex conjugate pairs. Pseudo-Hermiticity also increases the order of EPs in the parameter space [25]. H also has a chiral symmetry $\Gamma H \Gamma^{-1} = -H$, with the unitary transform $\Gamma = \mathrm{diag}(1, 1, -1, -1)$, which can be traced back from the time-reversal symmetry of the fluid Lagrangian. Equivalently, this chiral symmetry combined with the pseudo-Hermitian symmetry [Eq. (6)] can be taken into account as a pseudochiral symmetry

$$(\Gamma U) H (\Gamma U)^{-1} = -\bar{H}^\top, \tag{7}$$

that was also shown to constrain the existence of EPs [25]. We show that the combined effect of both pseudochirality and pseudo-Hermiticity leads to a codimension 2 for fourfold EPs (see SM [33]). This means that, for $N^2 < 0$, the four complex-valued eigenbands of H are expected to cross on a curve in the (K_r, S, L_ℓ) space. A direct derivation shows that those EPs satisfy

$$L_\ell = 0, \tag{8}$$

$$K_r^2 + S^2 = -N^2, \tag{9}$$

meaning that they form a circle of radius $|N|$ around the origin in the (K_r, S) plane at $L_\ell = 0$. H is diagonalizable everywhere apart from this circle, where only two eigenvectors exist, $(1 \quad 0 \quad 0 \quad 0)^\top$ and $(0 \quad 0 \quad (iK_r + S)/N \quad 1)^\top$. This *exceptional ring* thus consists of fourfold EPs (algebraic multiplicity of 4) with a geometric multiplicity of 2.

This ring where modes degenerate separates radial modes ($\ell = 0$) into two regions of distinct spectral properties. Figure 2 shows the real and imaginary parts of the eigenvalues of H. Outside the ring ($K_r^2 + S^2 > |N^2|$), the radial modes behave classically [37]: radial pressure waves have finite real frequencies and radial buoyancy modes have zero growth rates. Inside ($K_r^2 + S^2 < |N^2|$), they behave differently: the acoustic bands degenerate at $\Omega = 0$, and gravity modes have nonzero growth rates, the maximum value $\sqrt{-N^2}$ being reached for $K_r = S = 0$. When crossing the ring, two eigenvalues of H transit from real to pure imaginary values. Since H is pseudo-Hermitian, this can be interpreted as a Krein collision in the framework of Krein signature theory [38]. Unstable (imaginary) eigenvalues with zero Krein signature unfold from the encounter of stable (real) eigenvalues with opposite Krein quantities $\kappa(X) = \bar{X}^\top U X$, X being the corresponding eigenvector of H, colliding at the EP ring. A Krein quantity $\tilde{\kappa} = \int \mathrm{d}r\mathrm{d}\Phi\ (|\tilde{v}|^2 + |\tilde{w}|^2 + |\tilde{p}|^2 - |\tilde{\Theta}|^2)$, with Φ the solid angle, can also be defined for any solution $X(\boldsymbol{r}, t)$ of Eq. (1) and is a conserved quantity of the flow. In particular, $\tilde{\kappa} = 0$ for an unstable mode (see SM [33]).

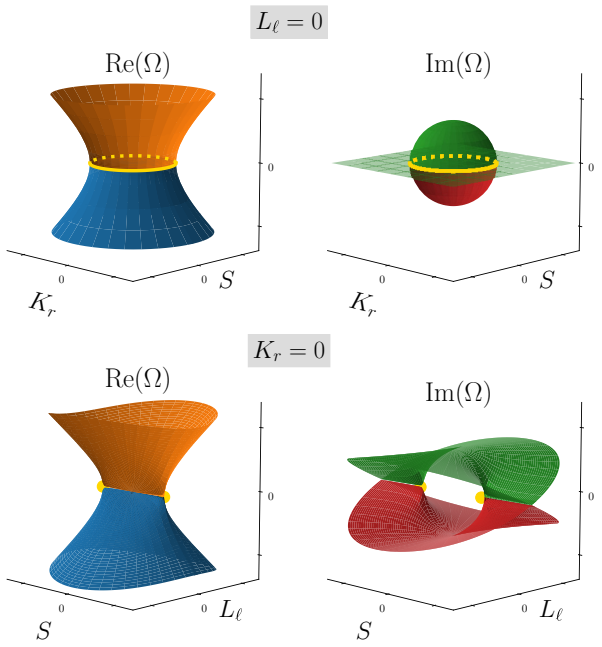

FIG. 2. Eigenvalues Ω of H around the EPs. There are two acoustic bands (orange and blue) with real eigenvalues, and two gravity bands (green and red) with purely imaginary eigenvalues. The yellow rings and points highlight the positions of the exceptional points. At large wavelengths $K_r \lesssim N$, pulsations and onset of convection behave very differently from what is expected in the short wavelength limit or in a Boussinesq approximation. Top right: Bubble of instability [39]. Bottom left: Double coffee filter [38]. Bottom-right: Viaduct [38].

To date, no theorem connects the EPs of the symbol matrix H to a possible manifestation in the spectrum of $\mathcal{H}$. If such a connection exists, one expects to find the footprint of EPs in radial modes ($\ell = 0$) as this is where the EP ring is found in the Wigner matrix, when the radial wavelength is large enough and the profiles of N^2 and S are such that the parameters cross the ring shown in Fig. 2 as r varies. Furthermore, the above analysis suggests that the relevant unstable modes are those of wavelengths typically longer than $\sim c_s/|N|$ ($N^2 \neq 0$ since convection has not started nor saturated to a quasiadiabatic state yet). This condition also requires S to be smaller than $|N|$, at least locally. Figure 3 shows the spectrum of a model where the aforementioned condition is satisfied. The unstable region

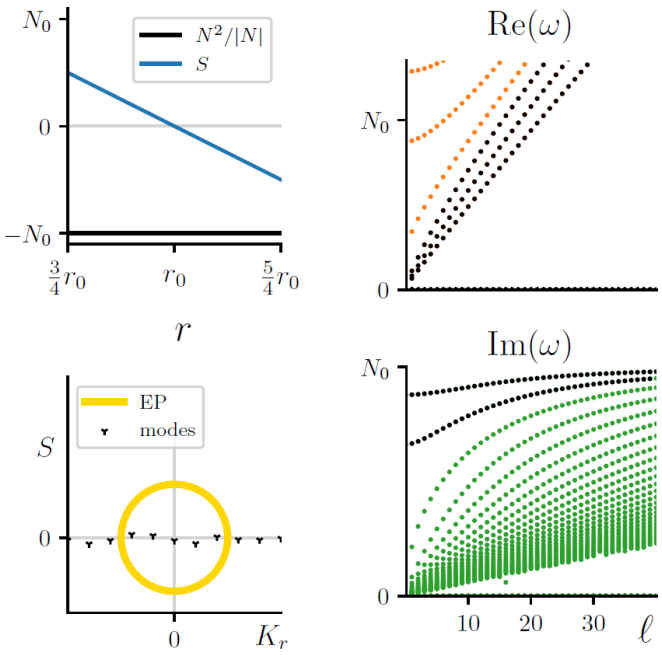

FIG. 3. Spectrum of a model with the stratification profile shown in the top left panel, corresponding to a layer $N^2 < 0$ such that S goes to zero at a given radius r_0 and remains smaller than $|N|$. Right panels: (i) Three acoustic modes with $\omega(\ell = 0) = 0$ and (ii) two gravity modes have nonzero growth rates in the $\ell = 0$ limit. The other modes have a classical behavior. Bottom left: Schematic of the location of the modes in parameter space: five modes behave differently because they are inside the EP ring. Orange points are acoustic modes, green points are unstable buoyancy modes, black points are exceptional modes. See SM for details on numerics [33].

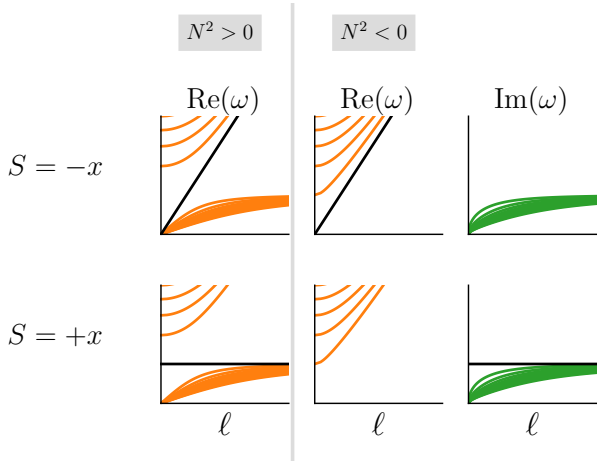

FIG. 4. Frequencies of models with S varying linearly in space (on some appropriately rescaled spatial variable x). Left: Stable stratification. The transiting mode depends on the sign of $\mathrm{d}S/\mathrm{d}x$. Right: Unstable stratification. Apart from the buoyancy modes being transposed to imaginary values, the transiting mode behaves as it does in the stable case. When $S = -x$, it arises as a propagating Lamb-like wave. When $S = +x$, it is an unstable mode of growth rate $|N|$, independently of ℓ. Only the first ten modes of each band are represented.

is wide enough so low-order radial modes have a sufficiently large radial wavelength, enough for the corresponding K_r to be located inside the ring. The spectrum exhibits three acoustic waves with zero frequency for $\ell \to 0$ and two unstable buoyancy modes with nonzero growth rates for $\ell \to 0$. Various profiles of preconvective unstable equilibria have been tested (Fig. 4 of SM [33]). They all have such exceptional modes since they are continuous deformations of the model of Fig. 3. Additional modes enter the EP ring by pairs when increasing the length of the layer. These properties are a physical footprint of the existence of EPs. These results are consistent with recent reports of experiments on compressible fluids, in which convection develops via axisymmetric modes [40–42].

Fundamental mode. In the stably stratified problem ($N^2 > 0$), H has degenerated eigenvalues for $(K_r, S, L_\ell) = (0, 0, \pm N)$, for which both the gravity and acoustic waves have frequencies N. Such degeneracies act as monopoles of Berry curvature in the parameter space (K_r, S, L_ℓ), and carry topological charges given by Chern numbers ± 1. Those Chern numbers are in direct correspondence with the existence of the Lamb-like waves in the spectrum of the operator $\mathcal{H}$, and explain the transit of the fundamental mode between the bands [4–6].

In the present Letter, H is no longer Hermitian, and the correspondence between the Lamb-like wave and the Chern numbers is not guaranteed. Several approaches have recently been developed to address the topological properties of non-Hermitian operators [27,29–31,43–50]. In particular, non-Hermitian formulations of the Chern numbers as monopoles of Berry curvature have been proposed, and a non-Hermitian generalization of the correspondence with the transit of the fundamental mode has been developed [26,51]. However, such a generalization cannot apply here, as the Hermitian degeneracy point is turned into a EP curve when the sign of N^2 is swapped, with zero net Chern number. Other works have introduced winding numbers associated to such circles of EPs [29,30,51], which we also find to vanish here. Nevertheless, we confirm below the existence of the the Lamb-like wave in regions with $N^2 < 0$. To do so, we study the normal form, setting linear spatial dependency for S, that is, $S(r) = \alpha(r - r_0)$, and $N^2 < 0$, sound speed c_s, and Lamb frequency L_ℓ constant [5,52]. The spectral properties of this problem capture the essential topology that will be reflected in the spectra of real objects. Within these assumptions, Eq. (1) is found to admit a fundamental mode with the zero node trapped around the radius r_0 where $S(r_0) = 0$. However, its behavior depends strongly on the slope of S at r_0, as shown in Fig. 4 (derivation in SM [33]). For a negative slope ($\alpha < 0$), this mode verifies $\omega^2 = L_\ell^2$ and its eigenfunctions are $\tilde{v}, \tilde{p} \propto \exp(-\frac{\alpha}{2c_s}(r - r_0)^2)$, $\tilde{w} = \tilde{\Theta} = 0$, which have the peculiar property of having no radial velocity nor entropy perturbation. This is the Lamb-like wave, and we thus conclude that it still propagates for $N^2 < 0$. In contrast, for a positive slope ($\alpha > 0$), the fundamental mode verifies $\omega^2 = -|N^2|$ and corresponds to a growing perturbation. Its eigenfunctions are $\tilde{v} = \tilde{p} = 0$, $\tilde{w}, \tilde{\Theta} \propto \exp(-\frac{\alpha}{2c_s}(r - r_0)^2)$, which have no angular velocity or pressure perturbation. We verified numerically that this mode is independent of the boundary conditions (see SM [33]). The importance of polarization relations is key

for wave topology [36,53,52]. Equation (1) admits nonzero solutions even if some of the component fields are equal to zero. Preserving the vector structure of the problem prevents the filtration of such solutions, as may happen when decoupling the initial system of equations into a single high-order ordinary differential equation. The general problem is expected to have the same properties, since it is a continuous deformation of this model, as long as no new location where S goes to zero is introduced (Fig. 4 of SM [33]). When $N^2(r)$ takes positive and negative values in different regions of the star, the Lamb wave still exists and coexists with an unstable buoyancy band. This is true whether $S(r)$ goes to zero inside the stable or unstable region. In sharp contrast, when the profile of $S(r)$ goes to zero with a positive slope in a region of negative N^2, we observe an unstable mode with a growth rate $\sim\sqrt{|N^2|}$, independently of ℓ.

Asteroseismology. The topological study of pulsating modes in stars has so far been restrained to radiative regions ($N^2 > 0$), the problem being Hermitian [5]. The question of whether the Lamb-type topological wave could propagate in convective regions (small $N^2 < 0$) remained unanswered. We show in this Letter that these waves can indeed propagate within them. They are therefore relevant even for objects such as high mass stars or Jupiter (see Fig. 1 of Ref. [5]). On top of this, convective regions can also generate multiple exceptional modes that behave like acoustic waves with zero frequency at $\ell = 0$. The existence or not of such modes in observational data constrains the internal structure of objects with convective interiors.

Birth of convection in protostars. Unstable exceptional modes of low radial order, low ℓ, and high growth rates develop when the conditions $N^2 < 0$ and $N^2 + S^2 < 0$ are satisfied. These conditions are met during the formation of a low-mass protostar, as shown in Fig. 1 from 2D simulations [23] (see SM [33] for physical interpretation). This clarifies the origin of radial unstable modes developing around the surface of the protostar. Hence, topological modes provide a possible explanation for the long-lasting problem of how and when convection starts in young stars. Further high-resolution 3D numerical simulations are, however, required to prove that the kinematic signature observed corresponds indeed to convective motion, and to study how these modes will develop in the nonlinear regime (e.g., convective eddies or fully developed turbulence).

Future studies are needed to quantify the role of rotation and self-gravity on these modes. Additional symmetries are expected to be broken in some regions of the extended parameter space. Exceptional points and Krein signature will be key tools to diagnose properties of global modes in such complex objects. The topological invariant associated with exceptional modes remains to be found.

Acknowledgments. We acknowledge funding from the ERC CoG Project PODCAST No. 864965. P.D. is supported by the national Grant No. ANR-18-CE30-0002-01. A.L. and L.J. are funded by a Contrat Doctoral Spécifique Normaliens. We thank A. Marie, G. Chabrier, E. Lynch, M. Rieutord, F. Lignières, B. Commerçon, I. Baraffe and A. Le Saux for useful comments and discussions.

[1] K. Schwarzschild, On the equilibrium of the Sun's atmosphere, Nachrichten von der Königlichen Gesellschaft der Wissenschaften zu Göttingen [Notices of the Royal Society of Science of Gttingen] Math.-phys. Klasse **195**, 41 (1906).

[2] R. Kippenhahn, A. Weigert, and A. Weiss, *Stellar Structure and Evolution* (Springer, Berlin, 1990), Vol. 192.

[3] D. Lecoanet and E. Quataert, Internal gravity wave excitation by turbulent convection, Mon. Not. R. Astron. Soc. **430**, 2363 (2013).

[4] M. Perrot, P. Delplace, and A. Venaille, Topological transition in stratified fluids, Nat. Phys. **15**, 781 (2019).

[5] A. Leclerc, G. Laibe, P. Delplace, A. Venaille, and N. Perez, Topological modes in stellar oscillations, Astrophys. J. **940**, 84 (2022).

[6] N. Perez, P. Delplace, and A. Venaille, Unidirectional modes induced by nontraditional coriolis force in stratified fluids, Phys. Rev. Lett. **128**, 184501 (2022).

[7] J. Bellisard. Change of the Chern number at band crossings, arXiv:cond-mat/9504030.

[8] Y. Hatsugai, Chern number and edge states in the integer quantum Hall effect, Phys. Rev. Lett. **71**, 3697 (1993).

[9] F. Faure and B. Zhilinskii, Topological Chern indices in molecular spectra, Phys. Rev. Lett. **85**, 960 (2000).

[10] G. M. Graf and M. Porta, Bulk-edge correspondence for two-dimensional topological insulators, Commun. Math. Phys. **324**, 851 (2013).

[11] P. Delplace, Berry-Chern monopoles and spectral flows, SciPost Phys. Lect. Notes 39 (2022).

[12] M. Z. Hasan and C. L. Kane, *Colloquium*: Topological insulators, Rev. Mod. Phys. **82**, 3045 (2010).

[13] J. B. Parker, J. B. Marston, S. M. Tobias, and Z. Zhu, Topological gaseous plasmon polariton in realistic plasma, Phys. Rev. Lett. **124**, 195001 (2020).

[14] J. B. Parker, Topological phase in plasma physics, J. Plasma Phys. **87**, 835870202 (2021).

[15] H. Qin and Y. Fu, Topological Langmuir-cyclotron wave, Sci. Adv. **9**, eadd8041 (2022)

[16] T. Ozawa, H. M. Price, A. Amo, N. Goldman, M. Hafezi, L. Lu, M. C. Rechtsman, D. Schuster, J. Simon, O. Zilberberg, and I. Carusotto, Topological photonics, Rev. Mod. Phys. **91**, 015006 (2019).

[17] L. Lu, J. D. Joannopoulos, and M. Soljačić, Topological photonics, Nat. Photonics **8**, 821 (2014).

[18] D. Xiao, M.-C. Chang, and Q. Niu, Berry phase effects on electronic properties, Rev. Mod. Phys. **82**, 1959 (2010).

[19] S. Huber, Topological mechanics, Nat. Phys. **12**, 621 (2016).

[20] L. M. Nash, D. Kleckner, A. Read, V. Vitelli, A. M. Turner, and W. T. M. Irvine, Topological mechanics of gyroscopic metamaterials, Proc. Natl. Acad. Sci. **112**, 14495 (2015).

[21] P. Delplace, J. B. Marston, and A. Venaille, Topological origin of equatorial waves, Science **358**, 1075 (2017).

[22] A. Venaille and P. Delplace, Wave topology brought to the coast, Phys. Rev. Res. **3**, 043002 (2021).

[23] A. Bhandare, R. Kuiper, T. Henning, C. Fendt, M. Flock, and G.-D. Marleau, Birth of convective low-mass to high-mass second Larson cores, A&A **638**, A86 (2020).

[24] A. A. Ahmad, M. González, P. Hennebelle, and B. Commerçon, The birth and early evolution of a low mass protostar, Astron. Astrophys. **680**, A23 (2023).

[25] P. Delplace, T. Yoshida, and Y. Hatsugai, Symmetry-protected multifold exceptional points and their topological characterization, Phys. Rev. Lett. **127**, 186602 (2021).

[26] L. Jezequel and P. Delplace, Non-Hermitian spectral flows and Berry-Chern monopoles, Phys. Rev. Lett. **130**, 066601 (2023).

[27] A. Ghatak and T. Das, New topological invariants in non-Hermitian systems, J. Phys.: Condens. Matter **31**, 263001 (2019).

[28] B. Zhen, C. W. Hsu, Y. Igarashi, L. Lu, I. Kaminer, A. Pick, S.-L. Chua, J. D. Joannopoulos, and M. Soljačić, Spawning rings of exceptional points out of Dirac cones, Nature (London) **525**, 354 (2015).

[29] Y. Xu and C. Zhang, Dirac and Weyl rings in three-dimensional cold-atom optical lattices, Phys. Rev. A **93**, 063606 (2016).

[30] D.-W. Zhang, Y. X. Zhao, R.-B. Liu, Z.-Y. Xue, S.-L. Zhu, and Z. D. Wang, Quantum simulation of exotic $\mathcal{PT}$-invariant topological nodal loop bands with ultracold atoms in an optical lattice, Phys. Rev. A **93**, 043617 (2016).

[31] F. K. Kunst, E. Edvardsson, J. C. Budich, and E. J. Bergholtz, Biorthogonal bulk-boundary correspondence in non-Hermitian systems, Phys. Rev. Lett. **121**, 026808 (2018).

[32] Z. Zhu, C. Li, and J. B. Marston, Topology of rotating stratified fluids with and without background shear flow, Phys. Rev. Res. **5**, 033191 (2023).

[33] See Supplemental Material at http://link.aps.org/supplemental/10.1103/PhysRevResearch.6.L012055 for details on derivations, calculations, and numerical tests. They additionally cite Refs. [54–64].

[34] P. Ledoux, Stellar models with convection and with discontinuity of the mean molecular weight, Astrophys. J. **105**, 305 (1947).

[35] T. G. Cowling, The non-radial oscillations of polytropic stars, Mon. Not. R. Astron. Soc. **101**, 367 (1941).

[36] Y. Onuki, Quasi-local method of wave decomposition in a slowly varying medium, J. Fluid Mech. **883**, A56 (2020).

[37] J. L. Tassoul, Sur l'instabilité convective d'une masse gazeuse inhomogène, [On the convective instability of a inhomogeneous gaseous mass], Annales d'Astrophysique **30**, 363 (1967).

[38] O. N. Kirillov, *Nonconservative Stability Problems of Modern Physics* (De Gruyter, Berlin, 2021), Vol. 14.

[39] R. S. MacKay, Stability of equilibria of Hamiltonian systems, in *Hamiltonian Dynamical Systems* (CRC Press, Boca Raton, 2020), pp. 137–153.

[40] R. Menaut, Y. Corre, L. Huguet, T. L. Reun, T. Alboussière, M. Bergman, R. Deguen, S. Labrosse, and M. Moulin, Experimental study of convection in the compressible regime, Phys. Rev. Fluids **4**, 033502 (2019).

[41] J. P. Koulakis and S. Putterman, Convective instability in a stratified ideal gas containing an acoustic field, J. Fluid Mech. **915**, A25 (2021).

[42] J. P. Koulakis, Y. Ofek, S. Pree, and S. Putterman, Thermal convection in a central force field mediated by sound, Phys. Rev. Lett. **130**, 034002 (2023).

[43] Z. Gong, Y. Ashida, K. Kawabata, K. Takasan, S. Higashikawa, and M. Ueda, Topological phases of non-Hermitian systems, Phys. Rev. X **8**, 031079 (2018).

[44] T.-S. Deng and W. Yi, Non-Bloch topological invariants in a non-Hermitian domain wall system, Phys. Rev. B **100**, 035102 (2019).

[45] S. Yao and Z. Wang, Edge states and topological invariants of non-Hermitian systems, Phys. Rev. Lett. **121**, 086803 (2018).

[46] D. S. Borgnia, A. J. Kruchkov, and R.-J. Slager, Non-Hermitian boundary modes and topology, Phys. Rev. Lett. **124**, 056802 (2020).

[47] Y. Ashida, Z. Gong, and M. Ueda, Non-Hermitian physics, Adv. Phys. **69**, 249 (2020).

[48] E. J. Bergholtz, J. C. Budich, and F. K. Kunst, Exceptional topology of non-Hermitian systems, Rev. Mod. Phys. **93**, 015005 (2021).

[49] H. Shen, B. Zhen, and L. Fu, Topological band theory for non-Hermitian Hamiltonians, Phys. Rev. Lett. **120**, 146402 (2018).

[50] T. E. Lee, Anomalous edge state in a non-Hermitian lattice, Phys. Rev. Lett. **116**, 133903 (2016).

[51] Y. Xu, S.-T. Wang, and L.-M. Duan, Weyl exceptional rings in a three-dimensional dissipative cold atomic gas, Phys. Rev. Lett. **118**, 045701 (2017).

[52] A. Venaille, Y. Onuki, N. Perez, and A. Leclerc, From ray tracing to waves of topological origin in continuous media, SciPost Phys. **14**, 062 (2023).

[53] N. Perez, P. Delplace, and A. Venaille, Manifestation of the Berry curvature in geophysical ray tracing, Proc. R. Soc. A **477**, 20200844 (2021).

[54] R. G. Barrera, G. A. Estevez, and J. Giraldo, Vector spherical harmonics and their application to magnetostatics, Eur. J. Phys. **6**, 287 (1985).

[55] K. J. Burns, G. M. Vasil, J. S. Oishi, D. Lecoanet, and B. P. Brown, Dedalus: A flexible framework for numerical simulations with spectral methods, Phys. Rev. Res. **2**, 023068 (2020).

[56] J. S. Oishi, K. J. Burns, S. E. Clark, E. H. Anders, Benjamin P Brown, G. M. Vasil, and D. Lecoanet, eigentools: A Python package for studying differential eigenvalue problems with an emphasis on robustness, J. Open Source Software **6**, 3079 (2021).

[57] D. O. Gough, Linear adiabatic stellar pulsation, in *Astrophysical Fluid Dynamics - Les Houches 1987*, edited by J.-P. Zahn, and J. Zinn-Justin, Vol. 49 (1993), p. 399.

[58] N. Vaytet, G. Chabrier, E. Audit, Benoît Commerçon, J. Masson, J. Ferguson, and F. Delahaye, Simulations of protostellar collapse using multigroup radiation hydrodynamics-ii. the second collapse, Astron. Astrophys. **557**, A90 (2013).

[59] H. Weyl, Quantum mechanics and Group theory, Z. Phys. **46**, 1 (1927).

[60] E. Wigner, On the quantum correction for thermodynamic equilibrium, Phys. Rev. **40**, 749 (1932).

[61] R. G. Littlejohn and W. G. Flynn, Geometric phases in the asymptotic theory of coupled wave equations, Phys. Rev. A **44**, 5239 (1991).

[62] C. Emmrich and A. Weinstein, Geometry of the transport equation in multicomponent WKB approximations, Commun. Math. Phys. **176**, 701 (1996).

[63] L. Ryzhik, G. Papanicolaou, and J. B. Keller, Transport equations for elastic and other waves in random media, Wave motion **24**, 327 (1996).

[64] J. Vanneste and T. G. Shepherd, On wave action and phase in the non–canonical Hamiltonian formulation, Proc. R. Soc. London, Ser. A **455**, 3 (1999).